HHS Public Access

Author manuscript

Bioenergy Res. Author manuscript; available in PMC 2020 June 15.

Published in final edited form as:

Bioenergy Res. 2019 June 15; 12: 409–418. doi:10.1007/s12155-019-09966-9.

Nanoparticle-mediated Impact on Growth and Fatty Acid Methyl Ester Composition in the Cyanobacterium *Fremyella diplosiphon*

Behnam Tabatabai[1], **Somayeh Gharaie Fathabad**[1], **Enock Bonyi**[2], **Sophia Rajini**[3], **Kadir Aslan**[2], **Viji Sitther**[1]

[1]Department of Biology, Morgan State University, 1700 East Cold Spring Lane, Baltimore, Maryland 21251, United States

[2]Department of Civil Engineering, Morgan State University, 1700 East Cold Spring Lane, Baltimore, Maryland 21251, United States

[3]Middle East Educational Services, Doha, Qatar, P.O. BOX: 3453

Abstract

Insufficient light supply is a major limitation in cultivation of cyanobacteria for scaled up biofuel production and other biotechnological applications, which has driven interest in nanoparticle-mediated enhancement of cellular light capture. In the present study, *Fremyella diplosiphon* wild type (Fd33) and halotolerant (HSF33–2) strains were grown in solution with 20, 100, and 200 nm-diameter gold nanoparticles (AuNPs) to determine their impact on biomass accumulation, pigmentation, and fatty acid methyl ester (FAME) production. Results revealed a significant increase in growth of Fd33 (0.244 ± 0.006) and HSF33–2 (0.112 ± 0.003) when treated with 200 nm AuNPs. In addition, we observed a significant increase in chlorophyll *a* accumulation in 200 nm AuNP-treated Fd33 (25.7%) and HSF33–2 (36.3%) indicating that NPs enhanced photosynthetic pigmentation. We did not observe any alteration in FAME composition and biodiesel properties of transesterified *F. diplosiphon* lipids among all AuNP treatments. Interactions between *F. diplosiphon* and AuNPs were visualized using scanning electron microscopy. Energy dispersive X-ray spectroscopy confirmed the presence of AuNPs outside cells with aggregation in high cell density locales. Our findings indicate that nanotechnological approaches could significantly enhance growth of the organism with no negative effect on FAME-derived biodiesel properties, thus augmenting *F. diplosiphon* as a potential biofuel agent.

Keywords

Biodiesel; Chlorophyll *a*; Energy dispersive X-ray spectroscopy; Gold colloids; Surface plasmon resonance

Introduction

Extensive use of coal and petroleum-derived fossil fuels has contributed to climate change, pollution, and other adverse environmental effects leading to higher fuel prices and the

*Corresponding Author.: viji.sitther@morgan.edu (V. Sitther).

depletion of non-renewable resources [1, 2]. These cumulative effects have driven great demand for new sources of biofuel, an emerging renewable alternative to fossil fuels. Of the various feedstocks, third-generation biofuel agents including algae and cyanobacteria are advantageous due to their ability to produce biogas, cellulosic ethanol, and biodiesel [3]. In particular, cyanobacteria are valuable platforms for such applications due to their fast generation time, minimal nutrient requirements, and high net energy converting biomass into fuel [4]. Among the various cyanobacterial species, *Fremyella diplosiphon* is an ideal candidate for biofuel production due to the presence of high-value fatty acid methyl esters (FAME) in its transesterified lipids [5]. With the incorporation of halotolerance in this organism, cultivation in brackish and marine waters with an average salinity of 35 g L^{-1} offers endless possibilities for utilization of mineral-rich sea water [6, 7].

The novelty of nanoparticle-enhanced photosynthesis is a unique design to enhance light capture in photosynthetic microorganisms using noble metal colloids [8, 9] that interact with light-inducing collective oscillations of the metal's electrons (surface plasmons) [10, 11]. This phenomenon has been reported to amplify and backscatter light at specific wavelengths resulting in a 30% increase of cell growth in microalgae/cyanobacteria [8]. Silver NPs and gold nanorods have been positioned around photobioreactors to enhance accumulation of chlorophyll and carotenoid pigments in the microalgae *Chlorella vulgaris* [12]. It has been reported that pigment accumulation in cyanobacteria is directly related to light wavelength and intensity [13] which is critical for efficient biomass production. In addition, NP suspensions can be recycled for more than five cycles without contamination, another factor that could further enhance cultivation efficiency in bioreactors [12].

Although the impact of metal NPs on microalgal/cyanobacterial biomass and pigment accumulation has been reported [8, 9, 12], there are no studies on their effect on *F. diplosiphon* growth and biodiesel properties. In the present study, we evaluated the impact of 20, 100, 200 nm-diameter gold NPs (AuNPs) on *F. diplosiphon* growth, pigment accumulation, FAME production, and biodiesel properties. In addition, the interactions of *F. diplosiphon* cells and AuNPs were visualized using scanning electron microscopy (SEM) and energy dispersive X-ray spectroscopy (EDS) to determine the locale of NPs.

Methods and Materials

Strain and Experimental Conditions

Wild type *F. diplosiphon* (Fd33) [14] was grown in liquid BG-11 medium containing 20 mM HEPES (BG-11/HEPES) [15] and halotolerant HSF33–2 [7] in liquid BG-11/HEPES supplemented with 35 g L^{-1} NaCl. Cultures were grown in vented 25 or 50 mL tissue culture flasks with continuous shaking at 70 rpm, 28 °C, and ambient CO_2 (350–1000 mg L^{-1}) in an Innova 44R incubator shaker (Eppendorf, Hamburg, Germany). The spectrum of the photosynthetic light bank in the shaker ranged from of 400–700 nm with peak wavelengths at 437 nm and 600–650 nm and an intensity adjusted to 30 μmol m^{-2} s^{-1} using the model LI-190SA quantum sensor (Li-Cor, Lincoln, NE, USA). Gold nanoparticles of 20, 100, and 200 nm-diameters (Sigma-Aldrich, St. Louis, MO, USA) with concentrations of 6.54×10^{11}, 3.84×10^{9}, and 1.9×10^{9} NP mL^{-1} respectively were used in this study.

Toxicity of 20, 100 and 200 nm AuNPs on *F. diplosiphon* Growth

The impact of AuNPs on *F. diplosiphon* growth was investigated to determine if localized surface plasmon resonance can be harnessed to enhance cultivation with minimal light input. *F. diplosiphon* Fd33 and HSF33–2 cultures were separately exposed to 20, 100, and 200 nm-diameter gold colloids at a 1:1 ratio of cyanobacterium: AuNPs and diluted to an initial optical density of 0.2 at 750 nm (OD_{750}) and a final volume of 24 mL (culture depth: 1.75 cm). In addition, *F. diplosiphon* grown in the absence of AuNPs (control) and AuNPs without bacteria (AuNP-) were examined to determine their effect. Cultures were grown over a 13 day-period as mentioned above and OD_{750} measured using an UV-Vis spectrophotometer (Agilent Technologies, Santa Clara, CA, USA) every 24 h for the first three days and every 48 h thereafter. Growth rate from Day 0 to peak OD_{750} of each strain was then calculated as doublings per day using the Least Fitting Squares method [16]. In addition, specific growth rate (μ) was calculated according to equation (1) and expressed as d^{-1} [17]. For both methods, replicate growth rates were derived separately and then averaged for each treatment.

$$\mu = \frac{\ln OD_{Final} - \ln OD_{Initial}}{\left(t_{Final} - t_{Initial}\right)} \quad (1)$$

Photosynthetic Pigment Extraction and Quantification

Chlorophyll *a* (chl*a*), carotenoids, and phycobiliproteins were extracted and quantified as previously described [18, 19] to test the impact of AuNPs on photosynthetic efficiency. *F. diplosiphon* cultures grown in liquid BG-11/HEPES were incubated on ice for 1 h, centrifuged at 13,000 × g for 5 min, and the supernatant removed. For extraction of chl*a* and carotenoids, flash frozen pellets resuspended in 90% methanol were incubated in dark at 4 °C for 1 h with rocking, centrifuged at 10,000 × g for 10 min, and the process repeated once. The supernatant was decanted, weighed, and OD_{470} and OD_{665} recorded to quantify carotenoids and chl*a* respectively. For extraction of phycobiliproteins, a second set of pellets was resuspended in 1 ml STES (50 mM Tris-HCl, 50 mM NaCl, 10 mM EDTA, 250 mM sucrose) containing lysozyme and incubated in dark at room temperature for 30 min with rocking. Cells were centrifuged at 13,000 × g for 5 min at room temperature and the supernatant measured at $OD_{565,}$ OD_{620}, and OD_{650}. Phycobiliprotein levels were calculated according to the procedure described previously [19] and reported relative to chl*a* [20].

Simultaneous Transesterification and Extraction

To investigate the effect of AuNPs on *F. diplosiphon* fatty acid profile, cultures were scaled up to 48 mL (culture depth: 1.75 cm), grown under culture conditions described above, and total cellular lipids subjected to direct transesterification [21]. Lyophilized cells were dissolved in 2 mL methanol with sulfuric acid and the reaction mix microwaved at 80 °C at 200 psi for 20 min in a multimode commercial scientific reaction microwave (CEM Corp, Matthews, NC, USA). After addition of chloroform, the mixture was washed with distilled water and centrifuged at 2000 rpm for phase separation. The organic layer containing FAMEs was isolated and the remaining biomass washed twice with chloroform and pooled.

Gas Chromatography-Mass Spectrometry and Theoretical Biodiesel Properties of AuNP-treated *F. diplosiphon* cells

Fatty acid composition of transesterified material was determined using Shimadzu GC17A/QP5050A gas chromatography-mass spectrometry (GC-MS) combination (Shimadzu Instruments, Columbia, MD, USA) at the Mass Spectrometry Facility at Johns Hopkins University (Baltimore, MD, USA). The GC17A was equipped with a low polarity (5% phenyl-, 95% methylsiloxane) capillary column (30 m length, 0.25 mm ID, 0.25 μm film thickness, and 10 m length guard column). In this process, products were dissolved in chloroform and 1 μL injected into the instrument using an autosampler. The injector temperature and transfer interface were maintained at 280 °C. The oven temperature was ramped from 130 °C (hold 10 min) to 160 °C (hold 7 min); 160 °C to 190 °C (hold 7 min), from 190 °C to 220 °C (hold 22 min) and from 220 °C to 250 °C (hold 17 min) at a rate of 10°C min^{-1} for each step [22]. The QP5050A is an EI quadrupole based mass spectrometer with a maximum scan range of m/z 40 to 900 and an ionizing electron energy of 70 eV. Peak identification was accomplished by comparing mass spectra to the American Oil Chemists Society Lipid Library Spectra of FAME. Three biological replicates of each sample were maintained. In addition, biodiesel properties of the transesterified lipids were theoretically analyzed from FAME composition (w%) using BiodieselAnalyzer© software Version 2.2 [23].

Fourier-transform Infrared Spectroscopy of *F. diplosiphon*

Total transesterified lipids from control and nano-treated cultures were subjected to Fourier-transform infrared spectroscopy (FTIR) using a Cary 630 FTIR spectrometer (Agilent Technologies, Santa Clara, CA, USA) to further confirm that FAME structure and composition were not affected by exposure to AuNPs. Parameters for FTIR measurements were as follows: a spectral range of 4000 – 400 cm^{-1}, 32 scans (approximately 15 s measurement time), and a spectral resolution of 4 cm^{-1}.

SEM and EDS Studies of *F. diplosiphon*-AuNP interactions

The interaction between *F. diplosiphon* cells and AuNPs was visualized using SEM and EDS analysis using a Hitachi 5500 scanning/scanning tunneling electron microscope (Hitachi, Ltd., Tokyo, Japan) and desktop SEM Phenom XL (Nanosciences Inc., Alexandria, VA, USA) equipped with EDS capability. Elemental analysis was performed using Phenom ProSuite Elemental Identification software at an acceleration voltage beam of 15 keV, resolution of 200 μm, and magnification up to 17000x to confirm the presence and location of AuNPs.

Statistical Analysis

Growth, photosynthetic pigment accumulation, and FAME studies were performed individually as three biological replicates per treatment from separate *F. diplosiphon* cultures and repeated once. Results were reported as cumulative treatment mean ± standard error. Statistical significance was determined using one-way analysis of variance and Tukey's Honest Significant Differences post-hoc test at 95% confidence intervals ($p < 0.05$). The single factor, fixed effect ANOVA model, $Y_{ij} = \mu + \alpha N_i + \varepsilon_{ij}$, was used where Y represents a

single, distinct parameter (growth rate, pigment level, or FAME content) in AuNP treatment i and biological replicate j. The μ represents overall mean adjusted by effects associated with AuNP treatment ($\alpha_i N$), and ε_{ij} is the experimental error from AuNP treatment i and biological replicate j.

Results and Discussion

Maximal *F. diplosiphon* Growth in Cultures Treated with 200 mm AuNPs

A major challenge to the establishment of sustainable, scaled up algal/cyanobacterial biofuel production pathways is the efficient cultivation of large biomass quantities, which mandates increased productivity while minimizing contamination [24, 25]. Several photobioreactor and pond designs for cultivation of microalgae are currently being tested, however these models are limited by factors such as gas transfer, mixing, light supply, and productivity [26]. In particular, lack of adequate light supply restricts uniform intensity and wavelength of light in a cultivation system, leading to reduced biomass [8]. Thus, the present approach aimed to minimize artificial light input to enhance cyanobacterial biomass accumulation in photobioreactors and pond systems.

Metal NP-derived surface plasmon resonance is a unique approach that has been identified to concentrate and scatter light, which reduces artificial light input [8, 12]. Previous studies have reported that surface plasmon resonance of gold and silver NPs can be employed to enhance microalgal and cyanobacterial growth using compartmentalized photobioreactors [8, 12]. However, this is the first report of a novel technique where cyanobacteria were cultivated in a single bioreactor with AuNPs, opening new possibilities for efficient cultivation. In our study, *F. diplosiphon* cells thrived when exposed to 20, 100, and 200 nm AuNPs at a 1:1 concentration indicating that AuNPs smaller than 200 nm were not toxic, unlike silver NPs which are lethal to cyanobacteria [27]. However, we observed significant increases ($Q= 5.45$; $p= 0.02$) (Table 1a; Online Resource 1a) in cultures treated with 200 nm AuNPs (0.244 ± 0.006) after nine days (peak growth) relative to the control (0.204 ± 0.002) (Fig. 1a). We detected significant growth ($Q= 4.84$ $p= 0.049$) (Table 1b; Online Resource 1b) in HSF33–2 cultures treated with 200 nm AuNPs (0.112 ± 0.003) compared to the control (0.072±0.001) after 11 days (peak growth) (Fig. 1b). In addition, calculation of specific growth rates confirmed significant increases in Fd33 ($Q= 5.87$; $p= 0.01$) and HSF33–2 ($Q= 9.463$; $p= 0.01$) treated with 200 nm AuNP relative to the untreated control (Online Resources 2–4). These findings indicate that exposure of *F. diplosiphon* to 200 nm AuNPs could be attributed to enhanced light capture and backscattering, thereby resulting in increased growth. A previous study reported strong backscattering of blue light from silver NPs leading to a 30% increase in *Chlamydomonas reinhardtii* and *Cyanothece* sp. cell growth [8]. We also observed cultures treated with 20 nm AuNPs to exhibit sustained cell growth up to 11 days (Fig. 1). By contrast, cultures treated with 100 and 200 nm AuNPs attained peak growth on the ninth day, suggesting prolonged generation time in *F. diplosiphon* cultivated with 20 nm AuNPs. We did not detect any growth in AuNP-treatments throughout the duration of the study confirming that AuNPs did not affect OD_{750} of cultures. Since we observed enhanced growth in cultures exposed to 200 nm AuNPs, this NP treatment was pursued for further studies.

Nano-treated *F. diplosiphon* Exhibit Enhanced chl*a* Accumulation

Since photosynthetic efficacy is directly related to biomass accumulation in cyanobacteria, it is imperative to determine the effect of AuNPs on pigment accumulation [28]. In photosynthetic microorganisms, the primary chlorophyll pigment chl*a* absorbs violet blue (410–430 nm) and red wavelengths (660 nm), and overlaps with the absorption spectra of AuNPs, suggesting that wavelengths altered by surface plasmon resonance could result in enhanced light supply [29–31]. We observed a significant increase in chl*a* accumulation in Fd33 (25.7%) and HSF33–2 (36.3%) (Fig. 2a) exposed with 200 nm AuNP suggesting enhanced cellular photosynthetic capacity. This can be attributed to AuNP-induced surface plasmon resonance scatter and amplification of available light, thus increasing light capture at effective wavelengths which could have enhanced chl*a* accumulation. Similar findings were reported by Eroglu et al. [12] where heightened backscattering of light by gold/silver NPs resulted in elevated chl*a* levels in the microalgae *Chlorella vulgaris*. On the contrary, we did not detect any significant differences in phycobiliprotein (Fig. 2b–d) and carotenoid (Fig. 2e) levels indicating that AuNPs did not directly affect pigment accumulation. It is interesting to note that phycobiliprotein accumulation is indirectly affected by AuNPs due to normalization to chl*a* levels. Despite comparable phycobiliprotein levels in control and AuNPs-treated cultures relative to chl*a* (Fig. 2b–d), higher absolute pigment accumulation was detected in nano-treated *F. diplosiphon*.

FAME Composition and Biodiesel Properties Unaltered in Nano-Treated Cultures

Previous efforts in our laboratory have demonstrated *F. diplosiphon* FAME production via direct transformation [5], thus it was imperative to determine the effect of AuNP treatment on FAME yield and composition. We did not detect significant changes in FAME composition of AuNP-treated *F. diplosiphon* transesterified lipids (Table 2, Fig. 3) indicating that AuNPs did not affect fatty acid composition or saturation ratio. These findings in concert with growth and pigmentation data suggest that AuNP treatment could enhance lipid productivity in a cultivation system. A recent study reported that an AuNP-containing photobioreactor increased lipid production to 1.5-fold in *C. reinhardtii* [32]. Additionally, we did not detect variation in the FTIR spectra of 200 nm AuNP-treated cultures relative to the control (Fig. 4), confirming that NPs did not affect FAME compositional and structural integrity. Our results suggest that AuNPs enhance light capture in *F. diplosiphon* with no negative effect on fatty acid profile that differentiates it as an intriguing candidate for biodiesel production.

To determine the effect of AuNPs on candidate biodiesel prospects, we calculated various chemical and physical properties of *F. diplosiphon* transesterified lipids. We did not observe any major changes in theoretical biodiesel properties of FAMEs from 200 nm AuNP-treated cultures (Table 3) confirming that this approach was not detrimental to the organism's biodiesel potential. Transesterified lipids from the AuNP-treated cultures maintained very high cetane numbers for both wild type (63.879) and halotolerant strains (65.132), which was comparable to untreated controls (63.373 and 63.490 respectively). By comparison, minimal American and European fuel standards for cetane number are 47 and 51 [33, 34] indicating that biodiesel from AuNP-treated cultures exceeded acceptable cetane levels. In addition, density (0.869–870 g/cm^3), viscosity (3.772–3.867 mm^2/s), and iodine (30.240–

37.590 g I_2/100 g) were unaffected and within the acceptable range. Additional features such cold filter plugging point (6.634–13.589 °C), cloud joint 26.884–29.461 °C), and pour point (22.363–25.160 °C) were very high in both strains as anticipated for fuel derived from highly saturated fatty acids (Table 3). These results suggest that blending the fuel to lower these values would be desirable for an ideal biodiesel product. Similar physical and chemical properties of *F. diplosiphon*-derived biodiesel were previously reported [5] suggesting that AuNP treatment did not alter the prospects of this organism as a biodiesel agent.

Validation of AuNP Aggregation Using SEM and EDS

We validated the presence of AuNPs in proximity to *F. diplosiphon* cell membranes using SEM (Fig. 5). We observed that AuNPs aggregated in locales populated with high cell density after nine days (Fig. 5f) suggesting that NPs enhance cyanobacterial growth. It is reported that AuNP aggregation has a variable effect on cellular uptake, indicating that a case-by-case evaluation is necessary to determine the effect of such interactions [30]. Our results revealed that aggregation of AuNPs did not result in uptake inside *F. diplosiphon* cells. Further, we observed Au peaks in EDS spectra of 200 nm AuNP-treated cultures confirming the occurrence and locale of NPs outside the cells (Fig. 5). Previously, SEM and EDS studies of AuNP-cyanobacterial cell interaction have shown “green synthesized” NPs [33, 35]; however, this is the first time that metal NP-cyanobacterial cell interactions were visualized to investigate surface plasmon-enhanced growth. Future studies using fluorescence tagging and imaging will be undertaken to determine NP entry into *F. diplosiphon* cells.

Conclusions

In summary, we demonstrate an innovative approach to augment *F. diplosiphon* growth by harnessing surface plasmon resonance of AuNPs as optical nanofilters. We detected no significant differences in FAME composition of total lipids in AuNP-treated subjected to direct transesterification, GC-MS, and FTIR spectroscopy. Theoretical chemical and physical properties derived from FAME profile confirmed that NP treatment did not alter the organism’s biodiesel potential. SEM and EDS studies confirmed the presence of AuNPs near *F. diplosiphon* cells, and NP aggregation was observed in areas with high cell density. These results suggest that nanotechnological approaches could augment biomass and chl*a* accumulation, thus minimizing artificial light costs in cyanobacterial cultivation systems.

Despite these findings, challenges to scalability remain, particularly with regard to cost of nanoparticles in a large-scale cultivation system. Currently, bulk AuNP purchases cost approximately $450/L, thus cost-effective methods via synthesis of these nanoparticles are being investigated. In addition, bioreactor designs that incorporate AuNPs in compartmentalized chambers and recycling of NPs will be evaluated in larger quantities to determine biofuel production pathways that maximize cost effectiveness.

Supplementary Material

Refer to Web version on PubMed Central for supplementary material.

Acknowledgements

The study was supported in part by the USDA NIFA [2016-67032-25007] and National Institutes of Health [UL1GM118973] awarded to Morgan State University. The authors thank Dr. Beronda L. Montgomery at Michigan State University for providing the Fd33 strain used in the study and Dr. Solomon Tadesse at Morgan State University for technical help in transesterification.

References

1. Quintana N, Van der Kooy F, Van de Rhee MD, Voshol GP, Verpoorte R (2011) Renewable energy from cyanobacteria: energy production optimization by metabolic pathway engineering. App Microbiol Biotechnol 91: 471–490
2. Martens P (2013) Health and climate change: modelling the impacts of global warming and ozone depletion, Routledge, London, UK: pp: 105–123
3. Machado IM, Atsumi S (2012) Cyanobacterial biofuel production. J Biotechnol 162: 50–56 [PubMed: 22446641]
4. Rodolfi L, Chini Zittelli G, Bassi N, Padovani G, Biondi N, Bonini G, Tredici MR (2009) Microalgae for oil: Strain selection, induction of lipid synthesis and outdoor mass cultivation in a low-cost photobioreactor. Biotechnol Bioengn 102: 100–112
5. Tabatabai B, Chen H, Lu J, Giwa-Otusajo J, McKenna AM, Shrivastava AK, Sitther V (2018) Fremyella diplosiphon as a biodiesel agent: Identification of fatty acid methyl esters via microwave-assisted direct in situ transesterification. Bioenergy Res DOI: 10.1007/s12155-018-9919-y.
6. Tabatabai B, Arumanayagam AS, Enitan O, Mani A, Natarajan SS, Sitther V (2017) Identification of a halotolerant mutant via in vitro mutagenesis in the cyanobacterium Fremyella diplosiphon. Curr Microbiol 74: 77–83 [PubMed: 27844126]
7. Tabatabai B, Arumanayagam AS, Enitan O, Mani A, Natarajan SS, Sitther V (2017) Overexpression of hlyB and mdh genes confers halotolerance in Fremyella diplosiphon, a freshwater cyanobacterium. Enzyme Microb Technol. 103: 12–17 [PubMed: 28554380]
8. Torkamani S, Wani SN, Tang YJ, Sureshkumar R (2010) Plasmon-enhanced microalgal growth in miniphotobioreactors. Appl Phys Lett 97: 043703
9. Ooms MD, Sieben VJ, Pierobon SC, Jung EE, Kalontarov M, Erickson D, Sinton D (2012) Evanescent photosynthesis: exciting cyanobacteria in a surface-confined light field. Phys Chem Chem Phys 14: 4817–4823 [PubMed: 22395147]
10. Kolwas K, Derkachova A, Shopa M (2009) Size characteristics of surface plasmons and their manifestation in scattering properties of metal particles. J Quant Spectrosc Radiat Transfer 110: 1490–1501
11. Kelly KL, Coronado E, Zhao LL, Schatz GC (2003) The optical properties of metal nanoparticles: the influence of size, shape, and dielectric environment. J Phys Chem B 107: 668–677
12. Eroglu E, Eggers PK, Winslade M, Smith SM, Raston CL (2013) Enhanced accumulation of microalgal pigments using metal nanoparticle solutions as light filtering devices. Green Chem 15: 3155–3159
13. Batschauer A (1998) Photoreceptors of higher plants. Planta 206: 479–492 [PubMed: 9821683]
14. Cobley JG, Zerweck E, Reyes R, Mody A, Seludo-Unson JR, Jaeger H, Weerasuriya S, Navankasattusas S (1990) Construction of shuttle plasmids which can be efficiently mobilized from Escherichia coli into the chromatically adapting cyanobacterium, Fremyella diplosiphon. Plasmid 30: 90–105
15. Allen MM (1968) Simple conditions for growth of unicellular blue- green algae on plates. J. Phycol 4: 1–4
16. Weisstein EW (2019) Least Squares Fitting--Exponential. MathWorld--A Wolfram Web Resource. http://mathworld.wolfram.com/LeastSquaresFittingExponential.html Accessed 28 Jan 2019.
17. Widdel F (2007) Theory and measurement of bacterial growth. Di dalam Grundpraktikum Mikrobiol. 4: 1–11
18. Kahn K, Mazel D, Houmard J, Tandeau de Marsac N, Schaefer M (1997) A role for cpeYZ in cyanobacterial phycoerythrin biosynthesis. J Bacteriol 179: 998–1006 [PubMed: 9023176]

19. Tandeau de Marsac N, Houmard J (1988) Complementary chromatic adaptation: physiological conditions and action spectra. Methods Enzymol 167: 318–328
20. Whitaker MJ, Bordowitz JR, Montgomery BL (2009) CpcF-dependent regulation of pigmentation and development in Fremyella diplosiphon. Biochem Biophys Res Commun 389: 602–606 [PubMed: 19748483]
21. Wahlen BD, Willis RM, Seefeldt LC (2011) Biodiesel production by simultaneous extraction and conversion of total lipids from microalgae, cyanobacteria, and wild mixed-cultures. Bioresour Technol 102: 2724–2730 [PubMed: 21123059]
22. Rosenberg JN, Kobayashi N, Barnes A, Noel EA, Betenbaugh MJ, Oyler GA (2014) Comparative analyses of three Chlorella species in response to light and sugar reveal distinctive lipid accumulation patterns in the microalga C. sorokiniana. PloS One 9: e92460 [PubMed: 24699196]
23. Talebi AF, Tabatabaei M, Christi Y (2014) BiodieselAnalyzer: a user-friendly software for predicting the properties of prospective biodiesel. Biofuel Res J 1: 55–57
24. Kim J, Yoo G, Lee H, Lim J, Kim K, Kim CW, Yang JW (2013) Methods of downstream processing for the production of biodiesel from microalgae. Biotechnol Adv 31: 862–876 [PubMed: 23632376]
25. Wijffels RH, Barbosa MJ (2010) An outlook on microalgal biofuels. Sci 329: 796–799
26. Pattarkine MV, Pattarkine VM (2012) Nanotechnology for algal biofuels In The Science of Algal Fuels pp: 147–163 Springer Netherlands
27. Burchardt AD, Carvalho RN, Valente A, Nativo P, Gilliland D, Garcìa CP, Passarella R, Pedroni V, Rossi F, Lettieri T (2012) Effects of silver nanoparticles in diatom Thalassiosira pseudonana and cyanobacterium Synechococcus sp. Environ Sci Technol 46: 11336–11344 [PubMed: 22958173]
28. Perrault SD, Chan WC (2009) Synthesis and surface modification of highly monodispersed, spherical gold nanoparticles of 50− 200 nm. J Amer Chem Soc 131: 17042–17043 [PubMed: 19891442]
29. Lichtenthaler HK, Buschmann C (2001) Chlorophylls and carotenoids: Measurement and characterization by UV-VIS spectroscopy. Curr Prot Food Analyt Chem 10.1002/0471142913.faf0403s01
30. Madigan CF, Lu MH, Sturm JC (2000) Improvement of output coupling efficiency of organic light-emitting diodes by backside substrate modification. Appl Phys Lett 76: 1650–1652
31. Hong S, Song M, Kim S, Bang D, Kang T, Choi I, Lee LP (2016) Integrated Microalgae Analysis Photobioreactor for Rapid Strain Selection. ACS Nano 10: 5635–5642 [PubMed: 27227421]
32. Albanese A, Chan WC (2011) Effect of gold nanoparticle aggregation on cell uptake and toxicity. ACS Nano 5: 5478–5489 [PubMed: 21692495]
33. Lengke MF, Fleet ME, Southam G (2006) Morphology of gold nanoparticles synthesized by filamentous cyanobacteria from gold (I)− thiosulfate and gold (III)− chloride complexes. Langmuir 22: 2780–2787 [PubMed: 16519482]
34. Masera K, Hossain AK (2017) Production, characterisation and assessment of biomixture fuels for compression ignition engine application. World Acad Sci Engn Technol Int J Mech Aero Indust Mech Manufact Engn 11: 1852–1858
35. Schrofel A, Kratosova G, Bohunicka M, Dobrocka E, Vavra I (2011) Biosynthesis of gold nanoparticles using diatoms—silica-gold and EPS-gold bionanocomposite formation. J Nano Res 13: 3207–3216

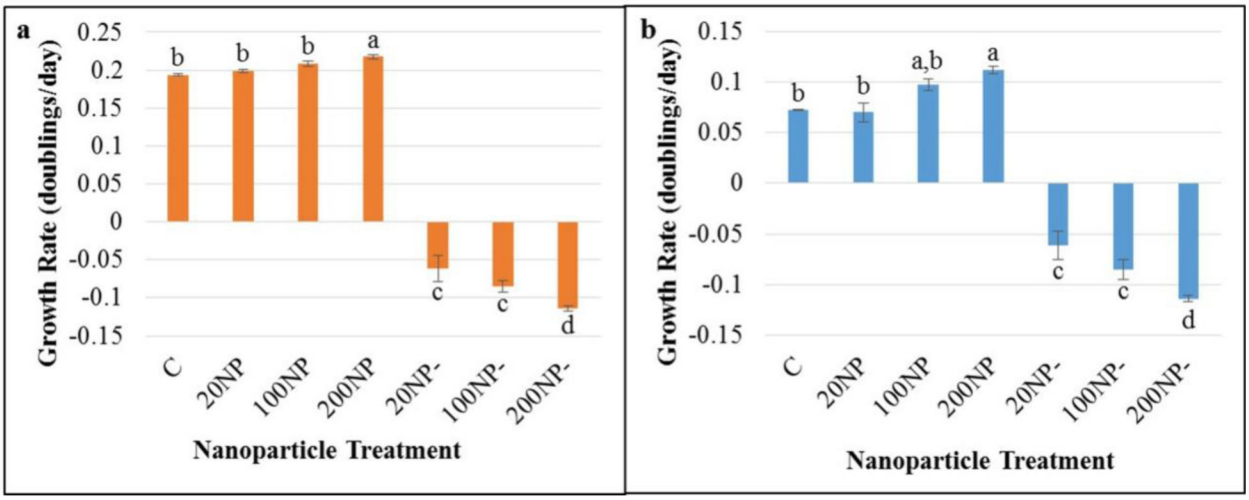

Fig. 1.

Least fitting squares-based growth rates of *Fremyella diplosiphon* **(a)** wild type (Fd33) and **(b)** halotolerant (HSF33–2) in solution with 20, 100, or 200 nm-diameter gold nanoparticles (NPs) over a period of 9 (Fd33) or 11 (HSF33–2) days. Cells grown in absence of AuNPs served as control (C) and gold colloids alone were denoted as AuNP only (NP-). Bars represent average growth rates (± standard error) for three biological replicates of each treatment. Different letters above bars indicate significance among treatment means at each time point ($p < 0.05$).

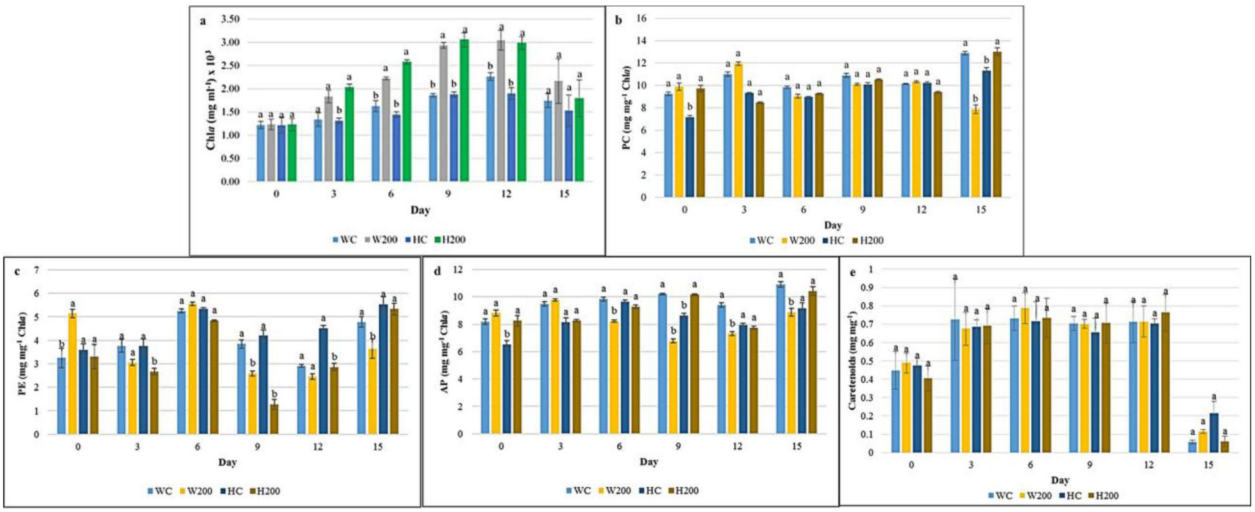

Fig. 2.

Impact of gold nanoparticles (AuNPs) on **(a)** chlorophyll *a* (chl*a*), **(b)** phycocyanin (PC), **(c)** allophycocyanin (AP), **(d)** phycoerythrin (PE), and **(e)** carotenoid accumulation in *Fremyella diplosiphon* wild type (Fd33) and halotolerant strain (HSF33–2). Treatments are as follows: wild type (W) Fd33 in the absence of AuNPs (WC) and in solution with 200 nm AuNP (W200); halotolerant (H) HSF33–2 in the absence of AuNPs (HC) and in solution with 200 nm AuNP (H200). Bars indicate average pigment accumulation (± standard error) for three biological replicates of each treatment. Different letters above bars denote significance among treatment means within each strain ($p < 0.05$).

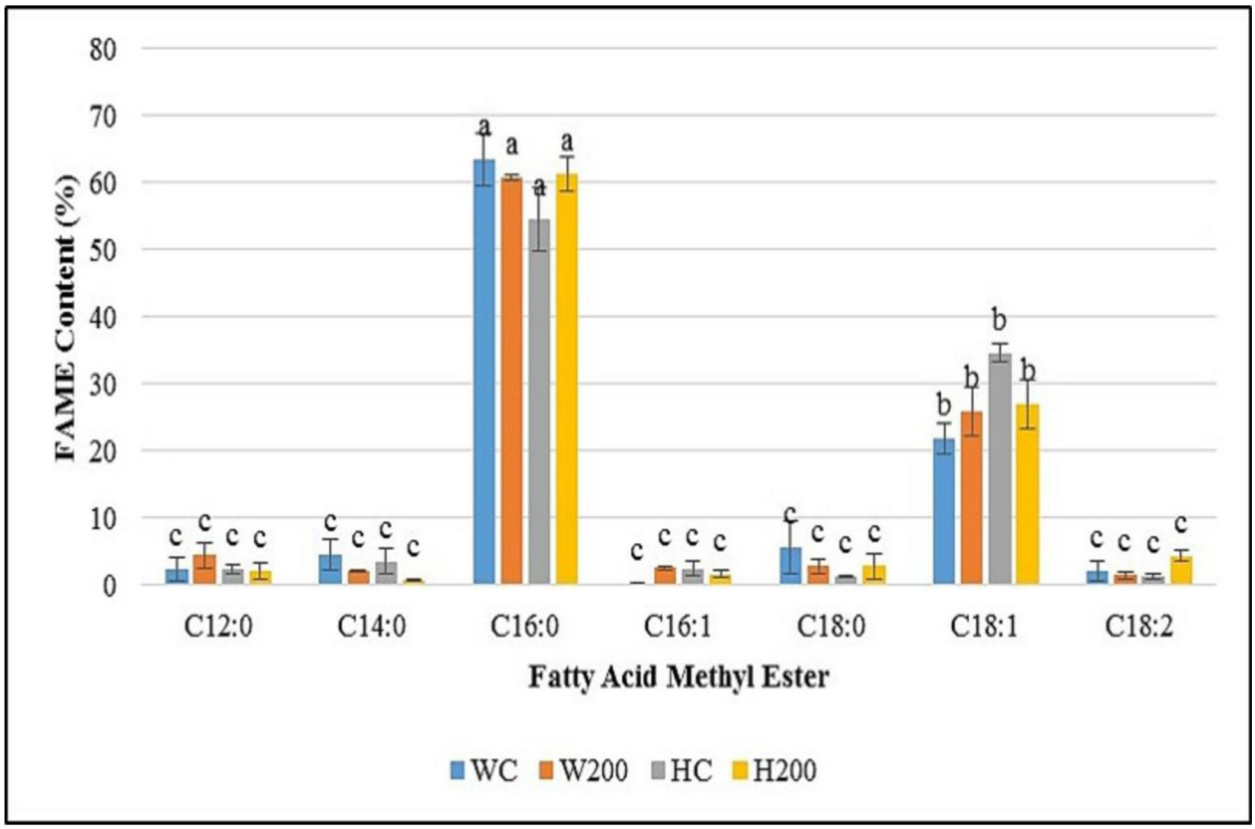

Fig 3.

Fatty acid methyl acid (FAME) composition of *Fremyella diplosiphon* wild type (Fd33) and halotolerant (HSF33–2) transesterified lipids grown in the absence of gold nanoparticles (AuNPs) and in solution with 200 nm AuNPs. Treatments are denoted as follows: Fd33 in the absence of AuNPs (WC) and in solution with 200 nm AuNPs (W200); HSF33–2 in the absence of NP (HC) and in solution with 200 nm AuNPs (H200). Bars represent average % relative content of FAME component (± standard error) for three biological replicates. Different letters above bars denote significance among treatment means within each strain ($p < 0.05$).

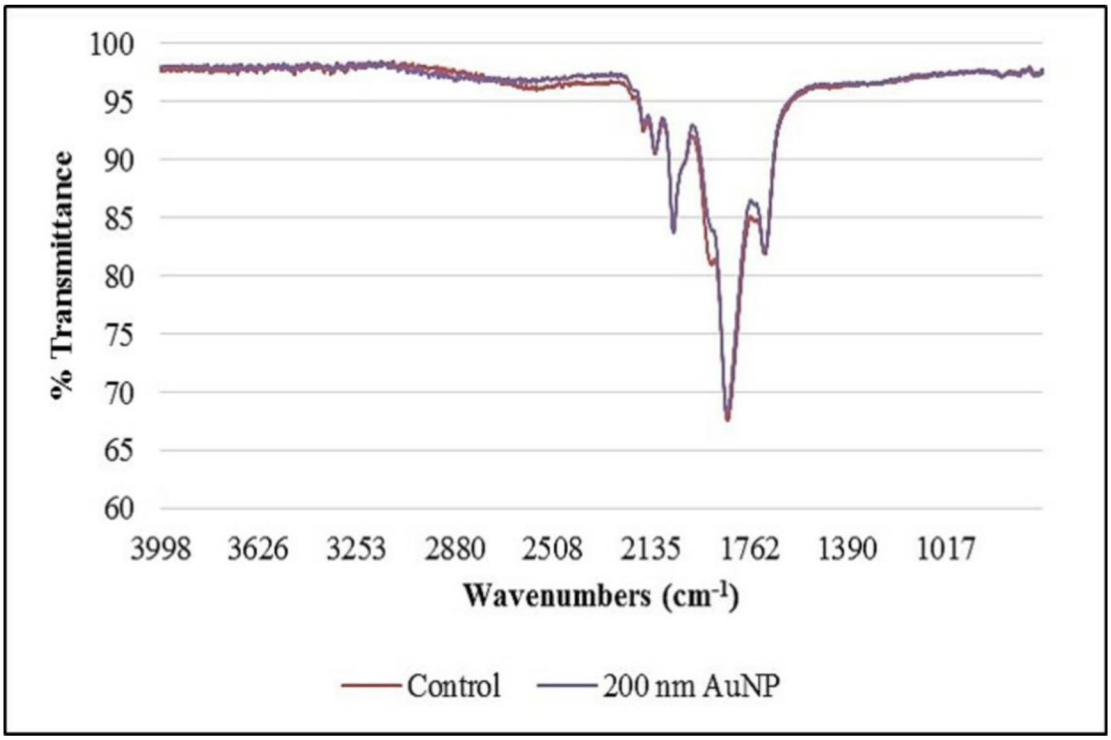

Fig. 4.

Fourier transform infrared (FTIR) spectroscopy of fatty acid methyl esters from *Fremylla diplosiphon* Fd33 (control) and cultures treated with 200 nm gold nanoparticles (200 nm AuNP).

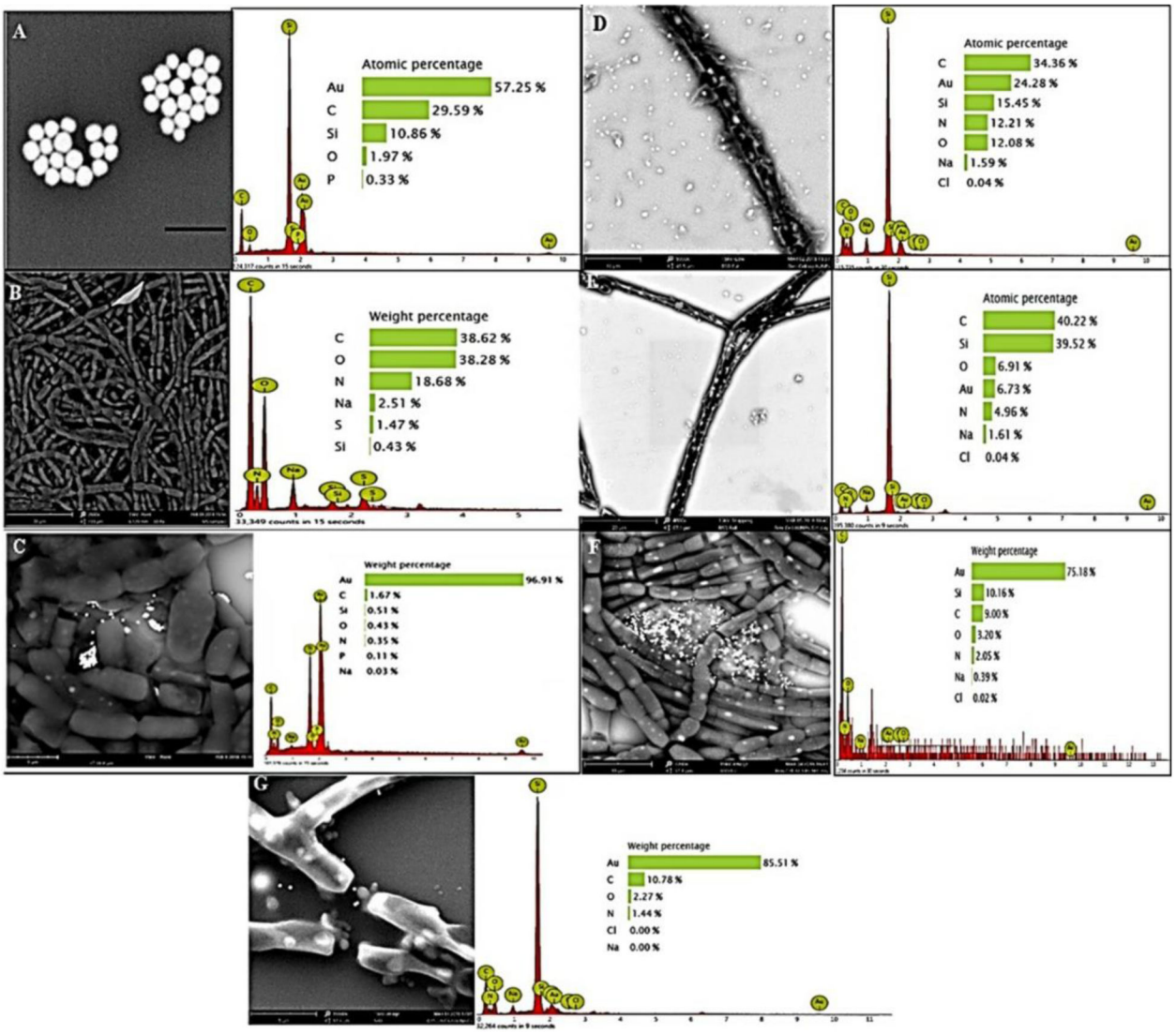

Fig. 5.

Scanning electron microscopy images and energy dispersive X-ray spectroscopy spectra of **(a)** 200 nm gold nanoparticles (AuNPs) **(b)** *Fremyella diplosiphon* filamentous cells (2500x), and cells in solution with 200 nm AuNP at **(c)** day 0, **(d)** day 3 (5500x), **(e)** day 6 (4000x), **(f)** day 9 (7200x), and **(g)** day 13 (15500x).

Table 1

Partitioning of variance for growth studies in *Fremyella diplosiphon* **(a)** wild type (Fd33) and **(b)** halotolerant (HSF33–2) strains using one-way class I analysis of variance.

(a)					
Source	**Sum of squares (SS)**	**Degrees of freedom (νν)**	**Mean square (MS)**	**F-statistic**	***p*-value**
Treatment	0.4753	6	0.0792	516.7167	1.33E-15
Error	0.0021	14	0.0002		
Total	0.4774	20			
(b)					
Source	**Sum of squares (SS)**	**Degrees of freedom (νν)**	**Mean square (MS)**	**F-statistic**	***p*-value**
Treatment	0.1711	6	0.0285	149.4665	7.10E-12
Error	0.0027	14	0.0002		
Total	0.1738	20			

Table 2

Fatty acid methyl ester (FAME) composition in *Fremyella diplosiphon* wild type (Fd33) and halotolerant (HSF33–2) strains based on relative abundance (% total extractable FAMEs).

Fatty Acid Methyl Ester	WC[a]	W200	HC	H200
Methyl dodecanoate (C12:0)	2.30	4.42	2.25	2.12
Methyl myristate (C14:0)	4.50	2.07	3.54	2.76
Methyl palmitate (C16:0)	63.53	60.85	64.62	61.35
Methyl hexadecanoate (C16:l)	0.12	2.51	2.43	1.66
Methyl octadecanoate (C18:0)	5.59	2.80	1.29	2.83
Methyl octadecenoate (C18:l)	21.87	25.90	24.62	26.91
Methyl octadecadienoate (C18:2)	2.09	1.44	1.25	2.37

[a]Treatments are as follows: Fd33 in the absence of AuNPs (WC) and in solution with 200 nm AuNPs (W200); HSF33–2 in the absence of AuNPs (HC) and in solution with 200 nm AuNPs (H200).

Table 3

Theoretical biodiesel properties of nano-treated *Fremyella diplosiphon* wild type (Fd33) and halotolerant (HSF33–2) strains transesterified lipids.

Biodiesel Properties	WC[a]	W200	HC	H200
Saponification Value (mg KOH/g fat)	213.783	211.617	213.693	212.903
Iodine Value (g I_2/100g)	37.590	36.500	37.116	30.240
Cetane number	63.373	63.879	63.490	65.132
Cold Filter Plugging Point (°C)	2.156	4.859	3.872	6.888
Cloud Point (°C)	24.066	26.300	24.805	28.739
Pour Point (°C)	19.304	21.729	20.106	24.377
Kinematic Viscosity (mm^2/s)	3.772	3.867	3.778	3.856
Density (g/cm^3)	0.870	0.870	0.870	0.869

[a]Treatments are as follows: Fd33 in the absence of AuNPs (WC) and in solution with 200 nm AuNPs (W200); HSF33–2 in the absence of AuNPs (HC) and in solution with 200 nm AuNPs (H200).